



**Environmental
Science**
Water Research & Technology

Comparing Energy Demands and Longevities of Membrane-based Capacitive Deionization Architectures

Journal:	<i>Environmental Science: Water Research & Technology</i>
Manuscript ID	EW-ART-03-2022-000188.R1
Article Type:	Paper

SCHOLARONE™
Manuscripts

WATER IMPACT STATEMENT

This study directly compares three different electrochemical cell designs used to desalinate water based on their energy demands and stabilities over time. A cell design that relied on a soluble redox-active compound to drive salt ion transport across membranes greatly outperformed cells that relied on electrode-based reactions to drive ion transport.

Comparing Energy Demands and Longevities of Membrane-based Capacitive Deionization Architectures

Vineeth Pothanamkandathil and Christopher A. Gorski*

Department of Civil and Environmental Engineering, The Pennsylvania State University,

*Corresponding author: Email: gorski@psu.edu; Tel: +1 814-865-5673

University Park, PA 16802, USA

ABSTRACT

Several capacitive deionization (CDI) cell architectures employ ion-exchange membranes to control the chemistry of the electrolyte contacting the electrodes. Here, we experimentally examined how exposing carbon electrodes to either a saline electrolyte or an electrolyte containing a soluble redox-active compound influenced deionization energy demands and long-term stability over ~50 hours. We specifically compared the energy demands ($W \cdot h \cdot L^{-1}$) required to deionize 20 mM NaCl to 15 mM with a 50% water recovery as a function of productivity ($L \cdot m^{-2} \cdot h^{-1}$). Relative to a conventional membrane capacitive deionization (MCDI) cell, flowing saline electrolyte over the electrodes did not affect energy demands but increased electrode salt adsorption capacities and capacity retention over repeated cycles. Exposing the electrodes to an electrolyte containing a redox-active compound, which made the cell behave similarly to an electro dialysis system, dramatically reduced energy demands and showed remarkable stability

over 50 hours of operation. These experimental results indicate that using a recirculated soluble redox-active compound in the electrolyte contacting the electrodes to balance charge leads to far more energy efficient brackish water deionization than when charge is balanced by the electrodes undergoing capacitive charging/discharging reactions.

INTRODUCTION

The deionization of water using electrochemical reactions has emerged as a promising alternative to reverse osmosis for treating brackish water (total dissolved solids = 500 – 10,000 mg·L⁻¹) at small scales due to its high degree of modularity and potentially low energy demands.(1-9) Within the literature, two main electrochemical deionization approaches exist. The first deionizes water primarily via electrode-based reactions in a process called capacitive deionization (CDI), and the second deionizes water primarily via selective ion transport across ion-exchange membranes in a process called electrodialysis (ED).(11) Modeling studies have indicated that conventional CDI systems have substantially higher energy demands than ED,(9, 12) but these results have been questioned in the literature due to concerns that values fed in the models predicted MCDI performance metrics that are lower than what are observed in experimental studies.(13-18)

While early CDI cells consisted of two capacitive electrodes in direct contact with the water being deionized,(7, 19-21) modern cells separate the feed water from the electrodes using ion-exchange membranes, as this modification tends to increase ion selectivity, faradaic efficiencies, and electrode stabilities.(7, 21-23) This cell design is known as membrane capacitive deionization (MCDI, **Figure 1**). To further improve the performance of MCDI cells, researchers have explored additional ways to integrate ion-exchange membranes into cells.(7, 24-42) One approach is to stack additional membranes between the electrodes, creating a system that resembles an ED cell.(43-45) This approach decreases energy demands, but increases cell construction costs, as the ion-exchange membranes are often the most expensive component in a cell.

An alternative approach that does not require more membranes is to expose the electrodes to an electrolyte that differs from the water being deionized. Researchers have explored using an aqueous electrolyte with a high salinity (i.e., multi-channel membrane capacitive deionization, MC-MCDI), suspended capacitive carbon particles (i.e., flow-electrode capacitive deionization, F-CDI), and/or soluble redox-active compounds (i.e., redox flow capacitive deionization, R-MCDI) (**Figure 1**).^(43-45, 47-53) Using a saline electrolyte can increase the electrodes' salt adsorption capacities and/or salt adsorption rates relative to those achieved in MCDI cells, while potentially decreasing deionization energy demands.^(43, 47) Recirculating the electrolyte and flowing it over both electrodes can also facilitate continuous cell operation.^(44, 49-53) In some cases, the addition of a soluble redox-active compound to the electrolyte decreased energy demands.^(49, 52) Note that systems using suspended carbon particles or a soluble redox-active

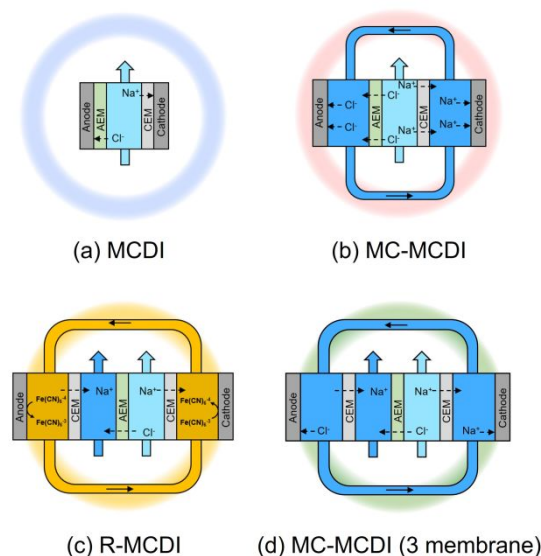


Figure 1. Schematic representation of (a) membrane capacitive deionization (MCDI), (b) multi-channel membrane capacitive deionization (MC-MCDI), (c) redox flow capacitive deionization (R-MCDI), and (d) MC-MCDI (three-membrane) architecture. Darker blue represents the concentrating stream, and lighter blue represents the deionizing stream. The yellow stream is

compound in a recirculated electrolyte begin to, or do, resemble ED cells, as salt is stored in the electrolyte, not at or in the electrode. In this manuscript, we refer to such cells using their naming conventions from the literature (i.e., MC-MCDI and R-MCDI), but they could also be described as modifications of ED.

While these new cell architectures have produced compelling salt adsorption capacities, salt adsorption rates, and/or low energy demands, the experimental results collected in different studies can rarely be directly compared because they were gathered under different feed water salinities, deionization rates, and/or deionization extents. Moreover, studies evaluating the feasibilities of these cell designs rarely reported the systems' stabilities over repeated cycles, which is important given that CDI cell lifetime is considered an important comparative metric to consider based on technoeconomic analyses.^(17, 55, 56) Therefore, the goal of this work was to experimentally compare membrane-based cell architectures in terms of energy demand and cell longevity. We performed the experiments under standardized deionization conditions (i.e., deionizing 20 mM NaCl to 15 mM with a 50% water recovery at different productivities). We compared the performances of a conventional MCDI system with systems in which the electrodes were exposed to a high salinity electrolyte (akin to MC-MCDI) or an electrolyte containing a soluble redox-active compound (akin to R-MCDI) (**Figure 1**). The cell designs akin to MCDI and MC-MCDI contained two ion-exchange membranes (**Figure 1**, panels **a** and **b**). The difference between these two was the MC-MCDI configuration had two outer channels containing recirculating 100 mM NaCl, whereas the MCDI configuration placed the membranes in direct contact with the electrodes. The cell akin to R-MCDI required one additional cation-exchange

membrane to prevent the redox-active compound (i.e., $[\text{Fe}(\text{CN})_6]^{4-}/[\text{Fe}(\text{CN})_6]^{3-}$) from being transported from the outer electrolyte channels to the feed water stream (**Figure 1c**). To fairly compare the R-MCDI and MC-MCDI cells, we tested a three-membrane MC-MCDI cell (**Figure 1d**) because stacking ion-exchange membranes is known to decrease energy demands.^(57, 58) The stabilities of the MCDI and MC-MCDI cells were measured by charging and discharging them over 250 cycles. The stability of the R-MCDI cell was measured by monitoring the cell voltage under a constant applied current because the cell did not require periodic discharging.

MATERIALS AND METHODS

All chemicals used in this study had a purity of 99% or higher. All experiments were conducted using deionized water (resistivity $\geq 18 \text{ M}\Omega\cdot\text{cm}$ at 25°C).

Electrode-current collector assembly: Activated carbon electrodes (PACMM 203, Material Methods, Irvine, CA, USA, 7 cm x 3 cm) were adhered to graphite current collectors (7 cm x 3 cm) to ensure proper contact between the electrode and the current collector. The adhesive was a slurry composed of conductive material (carbon black; Vulcan XC72R, Cabot, 75 wt% = 60 mg) and binder (polyvinylidene fluoride, PVDF; Kynar HSV 900, Arkema Inc., 25 wt% = 20 mg) suspended in 2.5 mL solvent (1-methyl-2-pyrrolidinone, Sigma-Aldrich). An aliquot of slurry (1 mL) which was painted on to the graphite current collector and the activated carbon electrode was placed on top of it. The electrode-current collector assembly was then dried at 70°C for 12 hours under vacuum in a vacuum oven. The electrodes were desiccated, then soaked in 100 mM NaCl solution for 24 hours before conducting deionization experiments.

All deionization experiments were performed in a custom fabricated flow-cell (**Section S1**). The cross-sectional area of the electrode exposed to the flow-stream was 21 cm² (7 cm x 3 cm). Procedures used for flow-cell assembly, deionization experiments, and longevity experiments are provided in **Section S1**. The deionization experiments were conducted in constant current mode. The voltage windows, flowrates, and applied currents used are in **Table S4**.

Energy demand and productivity calculations: The deionization performance of the three CDI architectures were compared based on their volumetric energy demand and throughput productivity. The volumetric energy demand (E_v , W·h·L⁻¹) was calculated as:

$$E_v = \frac{1}{V_D} \int I \cdot V(t) \cdot dt \quad (1)$$

where V_D was the volume of water deionized over the span of the deionization experiment, I was the applied current, $V(t)$ was the voltage across the cell as a function of time, and dt was the time step between two successive $V(t)$ measurements. Throughput productivity (P , L·m⁻²·h⁻¹) was calculated as:

$$P = \frac{V_D}{A \cdot t_{total}} \quad (2)$$

where A was the cross-sectional area of the electrode (21 cm²) and t_{total} was the total time taken for the deionization experiment. Detailed explanation on the procedure for energy demand, salt adsorption capacity, and productivity calculations are provided in **Sections S2 and S3**.

RESULTS AND DISCUSSION

Energy Demands for Deionization

We determined the volumetric energy demand required to deionize 20 mM NaCl to 15 mM in a single pass with a constant applied current for the four cell designs depicted in **Figure 1** under multiple flow rate-current density combinations (**Figure 2**). The volumetric energy demand of the MCDI and MC-MCDI cells were calculated using eq. 1 assuming complete energy recovery (i.e., 100% of the energy released during discharge was recovered). No energy could be recovered from the R-MCDI cell because the current direction was never switched. As expected, the volumetric

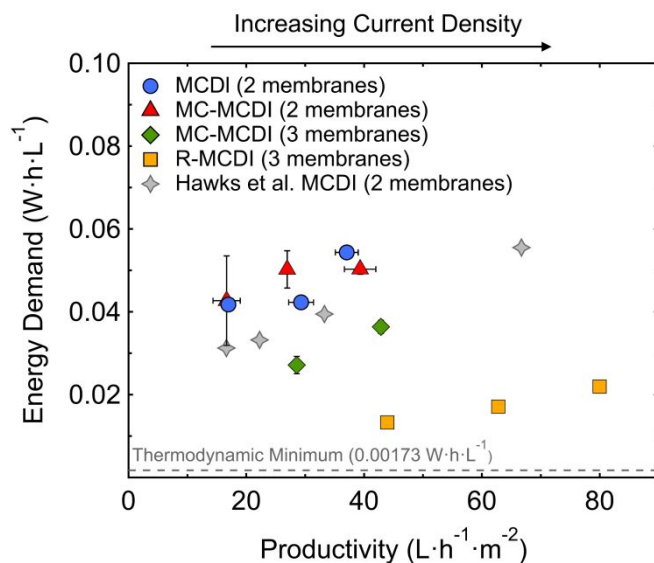


Figure 2. Energy demand versus productivity plot for the four cell architectures tested when deionizing 20 mM NaCl to 15 mM with a water recovery of 50%. Higher current densities were used to collect datapoints further to the right. The Hawks et al. MCDI (2 membranes) data is shown in panel A for comparison.⁴⁶ Each data point on the plot represents the average energy demand and productivity calculated based on two sets of experiments collected with fresh electrodes, and the error bars represent the range of values calculated. The MC-MCDI system had 100 mM NaCl solution circulating through the outer channel at the same flowrate as the

energy demand needed to deionize 20 mM NaCl to 15 mM was larger at higher productivities for all cell designs, as higher current densities were needed to achieve the required separation in a shorter time period (**Figure 2**). To benchmark the data collected here, we compared it to data reported for an MCDI cell deionizing 20 mM NaCl to 15 mM by Hawks et al. Our MCDI cell data yielded a slightly higher energy demand, which was likely due to our cell having a higher cell resistance (2.7 Ω at cycle 50, measured with EIS, see **Figure S7a** in **Section S4**) than what was reported in the previous study (1.2 Ω).

In our experiments, the two-membrane MCDI and MC-MCDI cells exhibited similar energy demand – productivity relationships (**Figure 2**). We attributed the modest differences between the two datasets to experimental error (i.e., minor differences in the cells each time they were assembled). The similar energy demands for the two configurations were consistent with the cells having the same faradaic efficiencies (both $\sim 100\%$, data not shown) and comparable cell resistances (MCDI: 2.7 Ω at cycle 50, MC-MCDI: 3.8 Ω at cycle 50; EIS data in **Figure S7**, panels a and b). The MC-MCDI cell resistance was slightly higher due to the cell having two additional outer-channels (each ~ 0.1 cm thick) that increased the distance between the two electrodes and possibly higher membrane resistances due to the larger concentration gradient. The performance metric that differed between the two cell designs was the salt adsorption capacity (SAC), with the MC-MCDI cell yielding higher SAC values than the MCDI cell. For example, under an applied current of 20 mA and flow rate of 3 mL \cdot min $^{-1}$, the SAC of the MC-MCDI cell was 8.14 ± 0.01 mg_{NaCl}/g_{electrode}, and the SAC of the MCDI cell 5.65 ± 0.13 mg_{NaCl}/g_{electrode}. (43, 47) The difference in SAC values is also apparent in the representative cell voltage plots of each cell, with the MC-

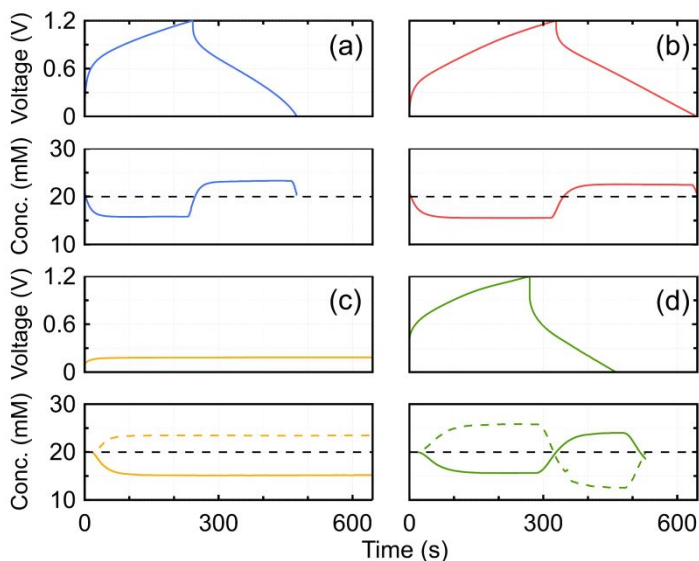


Figure 3. Representative plots of cell voltage and effluent concentration are shown as a function of time at a current of 20 mA and flow rate of 3 mL·min⁻¹ for **(a)** MCDI (2 membranes), MCDI cell taking longer to reach cutoff voltage (**Figure 3**, panels a and b). This observation indicates that increasing the SAC of an electrode did not decrease the energy required for the separation,⁽⁵⁸⁾ consistent with a previous derivation finding that energy demand values are independent of SAC values.⁽⁵⁹⁾ Note that the flow inefficiencies caused by the intermittent operation of MCDI and MC-MCDI systems would not have significantly altered the energy demands exhibited in **Figure 2** as the flow efficiencies calculated based on a previous study by Hawks et al. ranged between 0.90 and 0.98 for all conditions in this study.⁽⁶⁰⁾

The R-MCDI cell, which had an outer electrolyte containing equal concentrations of $\text{Fe}(\text{CN})_6^{3-}$ and $\text{Fe}(\text{CN})_6^{4-}$, produced far lower energy demands than the MCDI and MC-MCDI cells (**Figure 2**). This trend was due to two differences between the R-MCDI cell and the (MC-)MCDI cells. The first difference was that the R-MCDI cell had one more ion-exchange membrane than the MCDI and MC-MCDI cells. The R-MCDI cell required an additional cation-exchange

membrane to prevent $\text{Fe}(\text{CN})_6^{3-/4-}$ from leaving the outer electrolyte (**Figure 1c**). The stacking of ion-exchange membranes in this manner allowed the R-MCDI architecture to (1) operate continuously, which doubled the productivity of R-MCDI cell compared to two-membrane MCDI and MC-MCDI architecture, (2) avoided flow inefficiencies that can arise when operating intermittently,⁽⁶⁰⁾ and (3) allowed the cell to operate at lower current densities to achieve the same productivities. Stacking additional ion-exchange membranes is also known to decrease energy demands because they increase the number of salt ions transported across the membranes per electron transferred.^(57, 58) To facilitate a fairer comparison between the R-MCDI architecture and the (MC-)MCDI architectures, we constructed and tested a MC-MCDI cell having three ion-exchange membranes (**Figure 1d**). The inclusion of the third membrane cell increased the productivity and decreased the energy demand required to deionize the water (**Figure 2**). The energy demands for the three membrane MC-MCDI cell was, however, still substantially higher than the energy demands for the R-MCDI cell, indicating that the higher energy efficiency of the R-MCDI cell was not solely due to the cell containing a third ion-exchange membrane which enabled continuous operation.

To determine the other key difference between the cells, we evaluated each configuration's energetic losses. For all the cells, losses arose from cell resistance (i.e., the IR drop), which was a combination of the solution resistances in each channel, membrane resistances, and Donnan potentials across the ion-exchange membranes at a fixed current. The resistance of the R-MCDI cell (2.9Ω after 10 hours of operation, **Figure S7c**) was 38% lower than the three membrane MC-MCDI cell (4.7Ω , **Figure S7d**), indicating that the cell resistances contributed to the difference

in energy demands. Apart from the different resistances between the two cell architectures, the (MC-)MCDI cells also suffered from inefficient energy recovery (i.e., a portion of the energy used to charge the electrodes was not recovered during discharge). This loss was caused by the IR drop loss that occurs when the current direction is switched, the occurrence of charge redistribution within the electrodes, and parasitic faradaic reactions. (43, 61-64) In contrast, the R-MCDI cell did not have losses associated with imperfect energy recovery because the carbon electrodes did not undergo capacitive charging/discharging reactions and did not require the direction of current to be switched. For the R-MCDI cell, there was an additional possible loss associated with the overpotential required to drive the $\text{Fe}(\text{CN})_6^{3-/4-}$ redox cycling. Our results suggest that the losses associated with $\text{Fe}(\text{CN})_6^{3-/4-}$ redox cycling were far smaller than the losses associated with charging and discharging the capacitive carbon electrodes.

Overall, the R-MCDI system outperformed both the capacitive electrode-based MCDI systems in terms of energy demand. In fact, the energy demand for deionization with R-MCDI was similar to what was recently reported for a simulated full-stack (i.e., 500 cell) ED cell under similar operating conditions.(9, 65) The previous work estimated an energy demand of $0.013 \text{ W}\cdot\text{h}\cdot\text{L}^{-1}$ when deionizing $1 \text{ g}\cdot\text{L}^{-1}$ NaCl to $0.7 \text{ g}\cdot\text{L}^{-1}$ with a water recovery of 80% and a productivity of $20 \text{ L}\cdot\text{m}^{-2}\cdot\text{h}^{-1}$. We deionized $1.17 \text{ g}\cdot\text{L}^{-1}$ NaCl to $0.88 \text{ g}\cdot\text{L}^{-1}$ with a water recover of 50%. Extrapolating the data for R-MCDI from **Figure 2a** to a productivity of $20 \text{ L}\cdot\text{m}^{-2}\cdot\text{h}^{-1}$ yields a similar energy demand of $\sim 0.01 \text{ W}\cdot\text{h}\cdot\text{L}^{-1}$. The similar performances between the simulated full-stack ED cell and the three-membrane R-MCDI cells used here indicate that the voltage needed to drive the $\text{Fe}(\text{CN})_6$ oxidation and reduction reactions at the electrodes is effectively negligible. In other

words, the single-stack R-MCDI and full-stack ED cells have similar energy demands under the conditions studied because the energy demands in both systems are dominated by the ionic transport across ion exchange membranes and not the electrochemical reactions at the electrodes. Note that we used $\text{Fe}(\text{CN})_6^{3-/4-}$ as a redox couple based on its use in a past R-MCDI study and its simplicity.⁽⁵²⁾ We anticipate that the R-MCDI configuration could be improved by selecting alternative redox-active compounds with lower toxicities and/or faster electron transfer kinetics at the electrodes. Collectively, these findings indicate that separation based on ion transport across ion-exchange membranes, such as R-MCDI and ED, require lower energy demands compared to electrode-based separation, such as MCDI and MC-MCDI.⁽⁹⁾

Long-term stability

The long-term stabilities of the MCDI and two membrane MC-MCDI cells were evaluated based on charge storage capacity retention over 250 charge and discharge cycles (i.e., ~50 hours of constant operation under an applied current of 15 mA). The capacity of the MCDI cell began at $0.18 \text{ C}\cdot\text{m}^{-2}$ and decayed over 250 cycles to 45% of its initial capacity (**Figure 4a**), consistent with a longevity study performed on different carbon electrodes that lacked ion-exchange membranes. In contrast, the MC-MCDI cell had a higher initial capacity ($0.30 \text{ C}\cdot\text{m}^{-2}$, **Figure 4a**) and retained ~87% of its initial capacity over 250 cycles. The higher capacity retention of the MC-MCDI cell was likely due to the higher salt concentration in the electrolyte, which decreased the occurrence of parasitic electrode degradation reactions. Note the longevity test on the MC-MCDI configuration was performed without any binder between the electrode and the current collector because experiments performed with a binder led to probable binder dissolution that

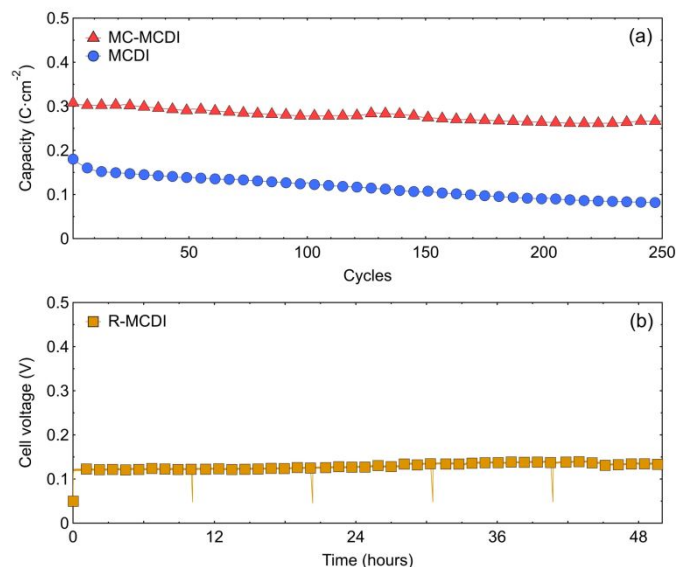


Figure 4. Capacity retention of (a) MCDI and two membrane MC-MCDI over 250 charge and discharge cycles at an applied constant current of 15mA. (b) Variation in cell voltage of R-MCDI system under constant current application (15mA) for 50 hours. The flowrate of the desalinating stream was 3 mL·min⁻¹ for all three architectures. 100 mM NaCl solution was circulated in the outer channels at a flowrate of 3 mL·min⁻¹ for the MC-MCDI system. A solution complicated data interpretation (see **Section S5** for details). The absence of a binder did not substantially affect the MC-MCDI cell resistance (with binder: 3.8 Ω, without binder: 4.2 Ω) because the electrode and spacer were tightly packed between the cation exchange membrane and current collector to facilitate pressure-based contact (refer to **Section S1** for detailed explanation of cell assembly). Note that the binder dissolution did not occur while performing the deionization tests and likely was only observed during the longevity tests because of the longer experimental time frame (i.e., 50 hours).

Unlike the MCDI and MC-MCDI cells, the stability and retention of the R-MCDI cell depended on the Fe(CN)₆^{3-/4-} maintaining its structure and being retained in the outer electrolyte channels. Therefore, we used the cell-voltage as a proxy for cell stability and Fe(CN)₆^{3-/4-} retention.

We measured the cell voltage when a constant current of 15 mA was applied to the flow-cell for 50 hours (**Figure 4b**). The R-MCDI showed a stable cell-voltage of 0.129 ± 0.006 V for the entire duration of the experiment (**Figure 4b**) indicating negligible $\text{Fe}(\text{CN})_6^{3-/4-}$ loss over 50 hours. A previous study conducted on an R-MCDI cell also observed negligible crossover of $\text{Fe}(\text{CN})_6^{3-/4-}$ redox couple.⁽⁵²⁾ From these data, we observed that the R-MCDI cell exhibited stable performance over 50 hours of continuous operation, while both the MCDI and MC-MCDI cells exhibited capacity degradation over the same period of time. Note that alternative redox-compounds can likely be found that exhibit lower crossovers than $\text{Fe}(\text{CN})_6^{3-/4-}$ if the R-MCDI system were optimized for long-term performance.

IMPLICATIONS

Several new membrane-based CDI architectures have recently been proposed primarily to decrease deionization energy demands. These approaches often utilize both electrode-based and ion-exchange membrane-based separations, making them effectively hybrids of CDI and ED. Among the architectures we tested, the addition of a soluble redox-active compound to the electrolyte in contact with electrode (R-MCDI) led to the largest decrease in energy demand while improving system stability. This modification effectively created an ED-like process where the salt removal capability of the system was decoupled from the salt adsorption capacity of the electrode. Our findings are consistent with ED being more energy efficient than CDI based on previous modelling work.⁽⁹⁾ Our results indicate that using a recirculated soluble redox-active compound in the electrolyte contacting the electrodes to balance charge leads to more energy efficient brackish water deionization than when charge is balanced by the electrodes undergoing

capacitive charging/discharging reactions. But, removing ion exchange membranes from CDI cells substantially increases energy demands.(46, 67) We opine that future work aiming to increase the viability of MCDI cell architectures that rely on capacitive reactions to store and release charge from electrodes without the use of redox-active compounds should search for inexpensive materials to perform ion selective charge transport across membranes that function in concert with the electrodes.(68-73)

ACKNOWLEDGEMENTS

Financial support for this study was provided by the National Science Foundation (CBET-1749207). Any opinions, findings, and conclusions or recommendations expressed in this material are those of the authors and do not necessarily reflect the views of the National Science Foundation. The authors thank Bruce Logan for providing valuable feedback during the writing process.

SUPPORTING INFORMATION

Detailed information on flow-cell assemblies, deionization experiments, longevity experiments, electrochemical impedance spectroscopy experiments, and energy demand analysis.

REFERENCES

1. Zhao R, Porada S, Biesheuvel PM, van der Wal A. Energy consumption in membrane capacitive deionization for different water recoveries and flow rates, and comparison with reverse osmosis. *Desalination*. 2013;330:35-41.
2. Welgemoed TJ, Schutte CF. Capacitive Deionization Technology™: An alternative desalination solution. *Desalination*. 2005;183(1):327-40.
3. Suss ME, Porada S, Sun X, Biesheuvel PM, Yoon J, Presser V. Water desalination via capacitive deionization: what is it and what can we expect from it? *Energy & Environmental Science*. 2015;8(8):2296-319.
4. Porada S, Zhao R, van der Wal A, Presser V, Biesheuvel PM. Review on the science and technology of water desalination by capacitive deionization. *Progress in Materials Science*. 2013;58(8):1388-442.
5. Oren Y. Capacitive deionization (CDI) for desalination and water treatment — past, present and future (a review). *Desalination*. 2008;228(1):10-29.
6. Landon J, Gao X, Omosibi A, Liu K. Progress and outlook for capacitive deionization technology. *Current Opinion in Chemical Engineering*. 2019;25:1-8.
7. Biesheuvel PM, van der Wal A. Membrane capacitive deionization. *Journal of Membrane Science*. 2010;346(2):256-62.
8. Anderson MA, Cudero AL, Palma J. Capacitive deionization as an electrochemical means of saving energy and delivering clean water. Comparison to present desalination practices: Will it compete? *Electrochimica Acta*. 2010;55(12):3845-56.
9. Patel SK, Qin M, Walker WS, Elimelech M. Energy Efficiency of Electro-Driven Brackish Water Desalination: Electrodialysis Significantly Outperforms Membrane Capacitive Deionization. *Environmental Science & Technology*. 2020;54(6):3663-77.
10. Biesheuvel P, Bazant M, Cusick R, Hatton T, Hatzell K, Hatzell M, et al. Capacitive Deionization--defining a class of desalination technologies. *arXiv preprint arXiv:170905925*. 2017.
11. Strathmann H. Electrodialysis, a mature technology with a multitude of new applications. *Desalination*. 2010;264(3):268-88.
12. Patel SK, Ritt CL, Deshmukh A, Wang Z, Qin M, Epsztein R, et al. The relative insignificance of advanced materials in enhancing the energy efficiency of desalination technologies. *Energy & Environmental Science*. 2020;13(6):1694-710.
13. Sharan P, Yoon TJ, Jaffe SM, Ju T, Currier RP, Findikoglu AT. Can capacitive deionization outperform reverse osmosis for brackish water desalination? *Cleaner Engineering and Technology*. 2021;3:100102.
14. Porada S, Zhang L, Dykstra JE. Energy consumption in membrane capacitive deionization and comparison with reverse osmosis. *Desalination*. 2020;488:114383.

15. Skuse C, Gallego-Schmid A, Azapagic A, Gorgojo P. Can emerging membrane-based desalination technologies replace reverse osmosis? *Desalination*. 2021;500:114844.
16. Pan S-Y, Haddad AZ, Kumar A, Wang S-W. Brackish water desalination using reverse osmosis and capacitive deionization at the water-energy nexus. *Water Research*. 2020;183:116064.
17. Hand S, Guest JS, Cusick RD. Technoeconomic Analysis of Brackish Water Capacitive Deionization: Navigating Tradeoffs between Performance, Lifetime, and Material Costs. *Environmental Science & Technology*. 2019;53(22):13353-63.
18. Ramachandran A, Oyarzun DI, Hawks SA, Campbell PG, Stadermann M, Santiago JG. Comments on "Comparison of energy consumption in desalination by capacitive deionization and reverse osmosis". *Desalination*. 2019;461:30-6.
19. Biesheuvel PM, Zhao R, Porada S, van der Wal A. Theory of membrane capacitive deionization including the effect of the electrode pore space. *Journal of Colloid and Interface Science*. 2011;360(1):239-48.
20. Porada S, Weinstein L, Dash R, van der Wal A, Bryjak M, Gogotsi Y, et al. Water Desalination Using Capacitive Deionization with Microporous Carbon Electrodes. *ACS Applied Materials & Interfaces*. 2012;4(3):1194-9.
21. Zhao R, Biesheuvel PM, van der Wal A. Energy consumption and constant current operation in membrane capacitive deionization. *Energy & Environmental Science*. 2012;5(11):9520-7.
22. Zhao R, Biesheuvel PM, Miedema H, Bruning H, van der Wal A. Charge Efficiency: A Functional Tool to Probe the Double-Layer Structure Inside of Porous Electrodes and Application in the Modeling of Capacitive Deionization. *The Journal of Physical Chemistry Letters*. 2010;1(1):205-10.
23. Tang W, He D, Zhang C, Kovalsky P, Waite TD. Comparison of Faradaic reactions in capacitive deionization (CDI) and membrane capacitive deionization (MCDI) water treatment processes. *Water Research*. 2017;120:229-37.
24. Yang J, Zou L, Song H, Hao Z. Development of novel MnO₂/nanoporous carbon composite electrodes in capacitive deionization technology. *Desalination*. 2011;276(1):199-206.
25. Myint MTZ, Dutta J. Fabrication of zinc oxide nanorods modified activated carbon cloth electrode for desalination of brackish water using capacitive deionization approach. *Desalination*. 2012;305:24-30.
26. Yin H, Zhao S, Wan J, Tang H, Chang L, He L, et al. Three-Dimensional Graphene/Metal Oxide Nanoparticle Hybrids for High-Performance Capacitive Deionization of Saline Water. *Advanced Materials*. 2013;25(43):6270-6.
27. Lee J, Kim S, Kim C, Yoon J. Hybrid capacitive deionization to enhance the desalination performance of capacitive techniques. *Energy & Environmental Science*. 2014;7(11):3683-9.
28. Omosebi A, Gao X, Landon J, Liu K. Asymmetric Electrode Configuration for Enhanced Membrane Capacitive Deionization. *ACS Applied Materials & Interfaces*. 2014;6(15):12640-9.

29. Li H, Zaviska F, Liang S, Li J, He L, Yang HY. A high charge efficiency electrode by self-assembling sulphonated reduced graphene oxide onto carbon fibre: towards enhanced capacitive deionization. *Journal of Materials Chemistry A*. 2014;2(10):3484-91.
30. Kim S, Lee J, Kim C, Yoon J. Na₂FeP₂O₇ as a Novel Material for Hybrid Capacitive Deionization. *Electrochimica Acta*. 2016;203:265-71.
31. Chen B, Wang Y, Chang Z, Wang X, Li M, Liu X, et al. Enhanced capacitive desalination of MnO₂ by forming composite with multi-walled carbon nanotubes. *RSC Advances*. 2016;6(8):6730-6.
32. Srimuk P, Kaasik F, Krüner B, Tolosa A, Fleischmann S, Jäckel N, et al. MXene as a novel intercalation-type pseudocapacitive cathode and anode for capacitive deionization. *Journal of Materials Chemistry A*. 2016;4(47):18265-71.
33. Porada S, Shrivastava A, Bukowska P, Biesheuvel PM, Smith KC. Nickel Hexacyanoferrate Electrodes for Continuous Cation Intercalation Desalination of Brackish Water. *Electrochimica Acta*. 2017;255:369-78.
34. Kim S, Yoon H, Shin D, Lee J, Yoon J. Electrochemical selective ion separation in capacitive deionization with sodium manganese oxide. *Journal of Colloid and Interface Science*. 2017;506:644-8.
35. Srimuk P, Lee J, Fleischmann S, Choudhury S, Jäckel N, Zeiger M, et al. Faradaic deionization of brackish and sea water via pseudocapacitive cation and anion intercalation into few-layered molybdenum disulfide. *Journal of Materials Chemistry A*. 2017;5(30):15640-9.
36. Chen F, Huang Y, Guo L, Ding M, Yang HY. A dual-ion electrochemistry deionization system based on AgCl-Na_{0.44}MnO₂ electrodes. *Nanoscale*. 2017;9(28):10101-8.
37. Lee J, Srimuk P, Aristizabal K, Kim C, Choudhury S, Nah Y-C, et al. Pseudocapacitive Desalination of Brackish Water and Seawater with Vanadium-Pentoxide-Decorated Multiwalled Carbon Nanotubes. *ChemSusChem*. 2017;10(18):3611-23.
38. Guo L, Mo R, Shi W, Huang Y, Leong ZY, Ding M, et al. A Prussian blue anode for high performance electrochemical deionization promoted by the faradaic mechanism. *Nanoscale*. 2017;9(35):13305-12.
39. Cao J, Wang Y, Wang L, Yu F, Ma J. Na₃V₂(PO₄)₃@C as Faradaic Electrodes in Capacitive Deionization for High-Performance Desalination. *Nano Letters*. 2019;19(2):823-8.
40. Ma X, Chen Y-A, Zhou K, Wu P-C, Hou C-H. Enhanced desalination performance via mixed capacitive-Faradaic ion storage using RuO₂-activated carbon composite electrodes. *Electrochimica Acta*. 2019;295:769-77.
41. Singh K, Porada S, de Gier HD, Biesheuvel PM, de Smet LCPM. Timeline on the application of intercalation materials in Capacitive Deionization. *Desalination*. 2019;455:115-34.
42. Tang W, Liang J, He D, Gong J, Tang L, Liu Z, et al. Various cell architectures of capacitive deionization: Recent advances and future trends. *Water Research*. 2019;150:225-51.

43. Kim C, Lee J, Srimuk P, Aslan M, Presser V. Concentration-Gradient Multichannel Flow-Stream Membrane Capacitive Deionization Cell for High Desalination Capacity of Carbon Electrodes. *ChemSusChem*. 2017;10(24):4914-20.
44. Kim N, Hong SP, Lee J, Kim C, Yoon J. High-Desalination Performance via Redox Couple Reaction in the Multichannel Capacitive Deionization System. *ACS Sustainable Chemistry & Engineering*. 2019;7(19):16182-9.
45. Jeon S-i, Yeo J-g, Yang S, Choi J, Kim DK. Ion storage and energy recovery of a flow-electrode capacitive deionization process. *Journal of Materials Chemistry A*. 2014;2(18):6378-83.
46. Hawks SA, Ramachandran A, Porada S, Campbell PG, Suss ME, Biesheuvel PM, et al. Performance metrics for the objective assessment of capacitive deionization systems. *Water Research*. 2019;152:126-37.
47. Lee J, Lee J, Ahn J, Jo K, Hong SP, Kim C, et al. Enhancement in Desalination Performance of Battery Electrodes via Improved Mass Transport Using a Multichannel Flow System. *ACS Applied Materials & Interfaces*. 2019;11(40):36580-8.
48. He C, Ma J, Zhang C, Song J, Waite TD. Short-Circuited Closed-Cycle Operation of Flow-Electrode CDI for Brackish Water Softening. *Environmental Science & Technology*. 2018;52(16):9350-60.
49. Wei Q, Hu Y, Wang J, Ru Q, Hou X, Zhao L, et al. Low energy consumption flow capacitive deionization with a combination of redox couples and carbon slurry. *Carbon*. 2020;170:487-92.
50. Wang J, Zhang Q, Chen F, Hou X, Tang Z, Shi Y, et al. Continuous desalination with a metal-free redox-mediator. *Journal of Materials Chemistry A*. 2019;7(23):13941-7.
51. Chen F, Wang J, Ru Q, Aung SH, Oo TZ, Chu B. Continuous Electrochemical Desalination via a Viologen Redox Flow Reaction. *Journal of The Electrochemical Society*. 2020;167(8):083503.
52. Chen F, Wang J, Feng C, Ma J, David Waite T. Low energy consumption and mechanism study of redox flow desalination. *Chemical Engineering Journal*. 2020;401:126111.
53. Thu Tran NA, Phuoc NM, Yoon H, Jung E, Lee Y-W, Kang B-G, et al. Improved Desalination Performance of Flow- and Fixed-Capacitive Deionization using Redox-Active Quinone. *ACS Sustainable Chemistry & Engineering*. 2020;8(44):16701-10.
54. Yang F, He Y, Rosentsvit L, Suss ME, Zhang X, Gao T, et al. Flow-electrode capacitive deionization: A review and new perspectives. *Water Research*. 2021;200:117222.
55. Liu X, Shanbhag S, Bartholomew TV, Whitacre JF, Mauter MS. Cost Comparison of Capacitive Deionization and Reverse Osmosis for Brackish Water Desalination. *ACS ES&T Engineering*. 2021;1(2):261-73.
56. Liu X, Shanbhag S, Natesakhawat S, Whitacre JF, Mauter MS. Performance Loss of Activated Carbon Electrodes in Capacitive Deionization: Mechanisms and Material Property Predictors. *Environmental Science & Technology*. 2020;54(23):15516-26.

57. Kim T, Gorski CA, Logan BE. Low Energy Desalination Using Battery Electrode Deionization. *Environmental Science & Technology Letters*. 2017;4(10):444-9.
58. Pothanamkandathil V, Fortunato J, Gorski CA. Electrochemical Desalination Using Intercalating Electrode Materials: A Comparison of Energy Demands. *Environmental Science & Technology*. 2020;54(6):3653-62.
59. Wang L, Dykstra JE, Lin S. Energy Efficiency of Capacitive Deionization. *Environmental Science & Technology*. 2019;53(7):3366-78.
60. Hawks SA, Knipe JM, Campbell PG, Loeb CK, Hubert MA, Santiago JG, et al. Quantifying the flow efficiency in constant-current capacitive deionization. *Water Research*. 2018;129:327-36.
61. Black J, Andreas HA. Effects of charge redistribution on self-discharge of electrochemical capacitors. *Electrochimica Acta*. 2009;54(13):3568-74.
62. Niu J, Conway BE, Pell WG. Comparative studies of self-discharge by potential decay and float-current measurements at C double-layer capacitor and battery electrodes. *Journal of Power Sources*. 2004;135(1):332-43.
63. Pell WG, Conway BE. Voltammetry at a de Levie brush electrode as a model for electrochemical supercapacitor behaviour. *Journal of Electroanalytical Chemistry*. 2001;500(1):121-33.
64. Conway BE. *Electrochemical supercapacitors: scientific fundamentals and technological applications*: Springer Science & Business Media; 2013.
65. Patel SK, Biesheuvel PM, Elimelech M. Energy Consumption of Brackish Water Desalination: Identifying the Sweet Spots for Electrodialysis and Reverse Osmosis. *ACS ES&T Engineering*. 2021;1(5):851-64.
66. He M, Fic K, Frąckowiak E, Novák P, Berg EJ. Influence of aqueous electrolyte concentration on parasitic reactions in high-voltage electrochemical capacitors. *Energy Storage Materials*. 2016;5:111-5.
67. Zhao Y, Wang Y, Wang R, Wu Y, Xu S, Wang J. Performance comparison and energy consumption analysis of capacitive deionization and membrane capacitive deionization processes. *Desalination*. 2013;324:127-33.
68. Zhang X, Zuo K, Zhang X, Zhang C, Liang P. Selective ion separation by capacitive deionization (CDI) based technologies: a state-of-the-art review. *Environmental Science: Water Research & Technology*. 2020;6(2):243-57.
69. Uwayid R, Guyes EN, Shocron AN, Gilron J, Elimelech M, Suss ME. Perfect divalent cation selectivity with capacitive deionization. *Water Research*. 2022;210:117959.
70. Hand S, Cusick RD. Emerging investigator series: capacitive deionization for selective removal of nitrate and perchlorate: impacts of ion selectivity and operating constraints on treatment costs. *Environmental Science: Water Research & Technology*. 2020;6(4):925-34.
71. Guyes EN, Shocron AN, Chen Y, Diesendruck CE, Suss ME. Long-lasting, monovalent-selective capacitive deionization electrodes. *npj Clean Water*. 2021;4(1):1-11.

72. Tsai S-W, Hackl L, Kumar A, Hou C-H. Exploring the electrosorption selectivity of nitrate over chloride in capacitive deionization (CDI) and membrane capacitive deionization (MCDI). *Desalination*. 2021;497:114764.
73. Kim T, Gorski CA, Logan BE. Ammonium Removal from Domestic Wastewater Using Selective Battery Electrodes. *Environmental Science & Technology Letters*. 2018;5(9):578-83.